Epigenetic upregulation of carotid body angiotensin signaling increases blood pressure.

Fengli Zhu M.Sc.[1], Zhuqing Wang Ph.D.[1], Kayla Davis B.Sc.[1], Hayden McSwiggin B.Sc.[1], Jekaterina Zyuzin Ph.D.[1], Jie Liu Ph.D.[1], Wei Yan M.D. Ph.D.[1, 2, 5], Virender K. Rehan M.D.[1, 3, 5], Nicholas Jendzjowsky Ph.D.[1, 4, 5*]

[1]The Lundquist Institute for Biomedical Innovation at Harbor-UCLA Medical Center, Torrance, CA 90502, USA
[2]Division of Metabolic Diseases and Translational Genomics, Harbor-UCLA Medical Center, Torrance, CA 90502
[3]Division of Neonatology, Harbor-UCLA Medical Center, Torrance, CA 90502, USA
[4] Division of Respiratory and Critical Care Medicine and Physiology, Harbor-UCLA Medical Center, Torrance, CA 90502, USA
[5]David Geffen School of Medicine, UCLA, Los Angeles, CA 90073, USA

Short title: Epigenetic programming of carotid bodies

*Corresponding Author: Nicholas Jendzjowsky, PhD
Rm 209 Martin Research Building,
The Lundquist Institute for Biomedical Innovation at Harbor-UCLA Medical Center
Division of Respiratory and Critical Care Medicine and Physiology
David Geffen School of Medicine, UCLA
1124 W Carson Street
Torrance, CA
90502-2006
Office:323-457-1663
Email: nicholas.jendzjowsky@lundquist.org

Total word count: 8853

Abstract

Epigenetic changes can be shaped by a wide array of environmental cues as well as maternal health and behaviors. One of the most detrimental behaviors to the developing fetus is nicotine exposure. Perinatal nicotine exposure remains a significant risk factor for cardiovascular health and in particular, hypertension. Increased basal carotid body activity and excitation are significant contributors to hypertension. This study investigated the epigenetic changes to carotid body activity induced by perinatal nicotine exposure resulting in carotid body-mediated hypertension. Using a rodent model of perinatal nicotine exposure, we show that angiotensin II type 1 receptor is upregulated in the carotid bodies of nicotine-exposed offspring. These changes were attributed to an upregulation of genetic promotion as DNA methylation of angiotensin II type 1 receptor occurred within intron regions, exemplifying an upregulation of genetic transcription for these genes. Nicotine increased angiotensin signaling *in vitro*. Carotid body reactivity to angiotensin was increased in perinatal nicotine-exposed offspring compared to control offspring. Further, carotid body denervation reduced arterial pressure as a result of suppressed efferent sympathetic activity in perinatal nicotine-exposed offspring. Our data demonstrate that perinatal nicotine exposure adversely affects carotid body afferent sensing, which augments efferent sympathetic activity to increase vasoconstrictor signaling and induce hypertension. Targeting angiotensin signaling in the carotid bodies may provide a way to alleviate hypertension acquired by adverse maternal uterine environments in general and perinatal nicotine exposure in particular.

Abstract word count: 229

Key words: Carotid body, sympathetic nervous activity, angiotensin, nicotine, epigenetic, developmental programming

50 **Introduction**

51 Adverse developmental programming is directly related to cardiovascular disease in later life.
52 The epigenetic modifications that occur in response to intra-uterine alterations have lasting
53 effects and are known to alter cardiovascular structure and function in response to several
54 environmental factors and maternal behaviors[1–5]. One of the most detrimental maternal behaviors
55 during the perinatal period, which can deleteriously predispose offspring to cardiovascular
56 diseases, is nicotine exposure, typically in the form of tobacco product use[6].

57 Perinatal tobacco smoke/nicotine exposure has been shown to augment blood pressure and
58 increase the risk of hypertension in later life[2,6,7]. Arteriolar wall thickening and increased
59 vasoconstrictor signaling are thought to be the primary causes of perinatal smoke/nicotine
60 exposure-induced hypertension[8–10]. Nicotine stimulates the renin-angiotensin-aldosterone
61 system[11] and increases both angiotensin-converting enzyme activity[12,13] as well as angiotensin II
62 type 1 receptor (AgtR1) expression and activity[12–14] within the aorta[15–17] and mesenteric
63 arterioles[16,18]. Such arteriolar reactivity would likely implement a hypertensive state.

64 Aberrant sympathetic nerve activity is significantly tied to cardiovascular disease and a prime
65 mediator of hypertension in a multitude of cardiometabolic diseases[19,20]. Carotid bodies are
66 polymodal sensors that regulate sympathetic nervous activity to control vasoconstriction to
67 regulate tissue oxygen/nutrient delivery[21,22]. Indeed, hypertension appears to be critically
68 dependent on tonic input from carotid bodies to augment sympathetic tone[19,20]. Carotid body
69 activity of nicotine-exposed offspring is not suppressed by hyperoxia, which typically quiesces
70 carotid body activity, suggesting an augmented basal sensitization[23,24]. Given their primary role
71 in stimulating arteriolar vasoconstriction[19,20] and their susceptibility to nicotine exposure[23,24], the
72 carotid bodies are likely susceptible to epigenetic modulation because of developmental

programming[25–27], which would lead to an elevation of tonic activity. Therefore, we investigated the hypothesis that carotid bodies are susceptible to epigenetic hypersensitization which results in increased blood pressure in perinatal nicotine-exposed offspring. To test our hypothesis, we engaged modern unbiased sequencing of RNA and DNA methylation of carotid bodies, tested signaling pathways *in vitro* and *in vivo,* and assessed the necessity of carotid bodies for heightened arterial pressure in perinatal nicotine-exposed pups.

Methods

Data availability

RNA sequencing and DNA bisulfite sequencing data have been deposited and can be found in the NIH SRA (Bioproject ID: PRJNA1106547). All other data are found in the supporting data and supplementary files and can be further made available upon request to the corresponding author.

Animal models, care and ethical standards

First-time pregnant Sprague-Dawley (SD) rat dams were purchased from Charles River (Hollister, CA) at gestational day 3. SD mothers were subject to subcutaneous nicotine injections (2mg/kg, Millipore Sigma, PHR2532) from gestational day 7 to post-natal day (PND) 21[28–30]. Control mothers received PBS (vehicle). Animals were housed with controlled temperature (21 ± 2 °C), humidity (55 ± 10%) and 12h light-dark cycle. Pups were weaned on post-natal day (PND) 21 and housed in pairs. Animals had unlimited access to food and water. Experiments on pups took place from PND56-80. All experimental procedures were approved by The Lundquist Institute for Biomedical Innovation at Harbor UCLA Medical Center IACUC board, protocol # 31659.

95 Assignment of control or nicotine to mothers was block randomized. Unbiased transcriptomic
96 and genomic sequencing was based on previous data acquired by neuronal sequencing results. *In*
97 *vitro* and *in vivo* power calculations were based on an estimated effect size of 50% difference
98 with assumed unified standard deviation across groups.

99 *PC12 culture*

100 PC12 cells were cultured in RPMI 1640 (Gibco # 11875093) supplemented with 10% Horse
101 Serum (Gibco Cat. #26050-088) and 5% fetal bovine serum (Gibco Cat. #F2442), 0.4µg/ml
102 dexamethasone (Millipore Sigma Cat. # D4902) and 1% penicillin/streptomycin (Millipore
103 Sigma Cat. # P0781). Cells were seeded at $3x10^5$ cells in 1ml of media per well (24 well plate,
104 qPCR) or 2500 cells in 150µl of media per well (96 well plate calcium imaging).

105 *Next-generation RNA sequencing*

106 On PND 56, animals were sedated (5% isoflurane, balance O2), exsanguinated and carotid
107 bodies gross dissected and placed in a sylgard-coated dissecting dish filled with Ham's F12
108 media. Carotid bodies were freed from the carotid bifurcation under a dissecting microscope.
109 Five carotid body pairs (n=10 carotid bodies from 5 rats) from each group and sex (n=5 rats per
110 group, per sex) were lysed and RNA was isolated using the easy-spin Total RNA extraction kit
111 (Boca scientific, Cat. # 17221). RNA purity was tested with Nanodrop spectrophotometer
112 (Thermofisher Cat. # ND2000USCAN) and deemed to be of appropriate quality when A260/280
113 was between 1.99 and 2.10. RNA sequencing was then conducted by an unbiased commercial
114 vendor (Novogene corporation, Sacramento CA), where further RNA purity was analyzed (RIN
115 >7) and downstream library construction took place.

116 *Whole genome DNA-bisulfite sequencing*

117 Carotid bodies were dissected as above. Five carotid body pairs (n=10 carotid bodies from 5 rats)
118 from each group and sex (n=5 rats per group, per sex) were lysed and DNA was isolated using
119 the QIAamp UCP DNA Micro Kit (Qiagen, Cat. # 56204). DNA purity was deemed sufficient
120 with A260/280 between 1.75-1.85. Bisulfite conversion and downstream whole-genome DNA-
121 bisulfite sequencing were conducted by (Novogene Corporation, Sacramento, CA).

122 *RNA qPCR*

123 For carotid bodies, an additional group of n=3 samples (n=5 rats per sample) from each group
124 was harvested as above, snap frozen and stored until analysis. Brain and kidneys were harvested
125 from each group of pups (one tissue per pup was deemed as n=1). For PC12 cells were washed in
126 PBS and then immediately lysed in lysis buffer and converted into cDNA. N=3 wells were
127 analyzed for each condition for each probe and five separate experiments were run. RNA was
128 converted to cDNA using the Tetro cDNA synthesis kit (Meridian life sciences, Cat. #
129 Bio65043). qPCR was conducted with Taqman specific probes. AgtR1a (Thermofisher
130 Rn02758772_s1), AgtR2 (Thermofisher Rn00560677_s1), angiotensinogen (Thermofisher
131 RN00593114_m1), angiotensin-converting enzyme (Thermofisher Rn00561094_m1), renin
132 (Thermofisher Rn02586313_m1), TH (Thermofisher Rn00562500_m1), endothelial PAS
133 domain-containing protein 1/ hypoxia inducible factor 2 alpha (EPAS1/Hif2α, Rn00576515_m1)
134 and TRPV1 (Thermofisher Rn00583117_m1). All experimental genes were evaluated in
135 reference to hypoxanthine-guanine phosphoribosyltransferase (HPRT Thermofisher
136 Rn01527840_m1). The qPCR reaction was completed using Taqman fast advanced master mix
137 enzyme (Thermofisher Cat. # 4444557) and the QuantStudio 3 thermocycler (Thermofisher Cat.
138 #A28567). Delta CT was calculated in reference to HPRT, and comparisons between groups
139 were made using an unpaired two-sided t-test.

140 *Methylated DNA immunoprecipitation-qPCR (MeDIP-qPCR)*

141 DNA was isolated from carotid bodies (n=4 per group, each n is comprised of carotid bodies
142 from 5 rats), brains and kidneys (n=4 rats per group, one tissue is n=1) and PC12 cells (1 well is
143 n=1). Carotid body and PC12 DNA was isolated using the QIAamp UCP DNA Micro Kit
144 (Qiagen, Cat. # 56204). Brain and kidney DNA was isolated using the Puregene Tissue kit
145 (Qiagen, Cat. # 158063). MeDIP was performed using the Methylated DNA
146 immunoprecipitation kit (Cat.# ab117133, Abcam) following the procedures described
147 previously[31]. Briefly, 100µL of the antibody buffer and 1µL anti-5-methylcytosine or reference
148 IgG antibody were added into wells and incubated at room temperature for 1 hour. During the
149 incubation, 1µg of genomic DNA was sheared between 200 and 1000 bp in the reaction buffer
150 using the Covaris M220 ultrasonicator, followed by denaturation at 95 °C for 2 minutes, then
151 placed on ice until use. An aliquot of 5 µL of the denatured DNA was saved as the input DNA.
152 The strip wells bound with antibodies were washed with 150µL of the antibody buffer and 150µL
153 of the wash buffer once, followed by incubation with the sheared DNA at room temperature for
154 2 hours. The antibody-enriched DNA was eluted in the DNA release buffer containing proteinase
155 K followed by DNA purification. qPCR was performed using Fast SYBR™ Green Master Mix
156 (Cat.# 4385612, Thermo Fisher Scientific) to identify DNA methylation levels. Primer sequence-
157 AgtR1: Forward TACCTAAACATAGTAAAAGCCAAACACA; AgtR1: Reverse
158 TATCCTGTTGATCTCTTTTTGTTGTCTG. ΔCt was calculated as Methylated AgtR1 DNA –
159 Total AgtR1 DNA and was used to plot the data[31,32]. Comparisons between groups were made
160 using an unpaired two-sided t-test.

161 *Immunohistochemistry*

162 Carotid bodies were gross dissected as above. Then they were cleaned from connective tissue but
163 left attached to the surrounding carotid artery bifurcation as previously[33]. Tissues were fixed in
164 4% paraformaldehyde for 1-2 hours at 4°C, then cryopreserved in 30% sucrose overnight at 4°C,
165 dried embedded in optimal cutting temperature compound (OCT) and cut at 14µm sections on a
166 cryostat. Sections were then washed (PBS), permeabilized (Triton x 20%) blocked with 10%
167 goat serum (Abcam, Cat. # ab7481), and incubated with antibodies for tyrosine hydroxylase (TH,
168 Millipore Sigma ZMS1033, clone 20/40/15), AgtR1 (Millipore Sigma AB15552, polyclonal) and
169 TRPV1 (Alomone Labs ACC-030, polyconal) for 24hours at 4°C and subsequently stained with
170 appropriate secondaries (Jackson Laboratories Goat-anti rabbit Cy3 111-165-003, Cy5 111-005-
171 003 and Goat-anti mouse 488 115-545-003) for 90 minutes and then counterstained with DAPI
172 (Millipore Sigma MBD0015) and coverslipped with prolong diamond antifade mounting media
173 (Thermofisher #P36970). Slides were imaged using the Leica Thunder imaging acquisition
174 system.

175 *Calcium imaging*

176 PC12 cells were separated into media (control), stimulated with nicotine (Sigma Cat. # 6019-06-
177 3, 50µg/ml), angiotensin II (Tocris Cat. # 1158, 5µM), nicotine + angiotensin II, angiotensin II +
178 losartan (Tocris Cat. # 3798, 3µM), nicotine + angiotensin II + losartan, angiotensin II +
179 AMG9810 (TRPV1 antagonist Tocris Cat. # 2316, 10µM), nicotine + angiotensin II +
180 AMG9810, or nicotine + angiotensin II + losartan + AMG9810, for 1 hour and then incubated
181 with Calcium Orange AM methyl ester (Invitrogen Cat. # C3015) + 0.01% Pluronic acid
182 (Invitrogen Cat. #F-127) for 20 minutes, washed in media and then imaged in the Incucyte
183 imaging system (Sartorius) using the Neural imaging parameters (Ex: 549λm/ Em: 576λm, 60s)

184 for 1 hour. The frequency of methyl ester excitation bursts was averaged for each well to express
185 a single value. Data were analyzed with One-way ANOVA using the Holm-Sidak post-hoc test.

186 *In vivo carotid body reactivity*

187 Rats from control or nicotine groups (as above) were tested on PND 56-58. Rats were
188 anesthetized with 5% isoflurane (balance room air) using the Kent Scientific Somnosuite
189 anesthesia system. The femoral artery and vein were cannulated, and the arterial line was
190 instrumented to a pressure transducer to measure continuous arterial pressure (AD instruments
191 MLT0670) using the PowerLab data acquisition console (AD instruments PL3516/P). The vein
192 was then connected to a syringe pump (Fisherscientific Cat. # 14831200) to induce a
193 15mg/kg/min infusion of alfaxan (Victor Medical Cat. # 1629020)[34,35]. Then the jugular vein was
194 cannulated to deliver bolus injections of Angiotensin II (Tocris Cat. # 1158 1mg/kg) and sodium
195 cyanide (NaCN, Fisherscientific Cat. # AA1213722, 200µg/kg). These injections were repeated
196 following bilateral carotid body denervation. Briefly, the neck area was shaved, and a midline
197 incision exposed the carotid artery. Then glands were pushed aside, and the carotid bodies were
198 identified within the carotid bifurcation, underneath the occipital artery. The carotid sinus nerve
199 was confirmed as it was traced to the glossopharyngeal nerve, then denervated, as previous[34].
200 Mean arterial pressure was averaged at the 60s preceding each bolus injection and a 60s average
201 during the peak reactive response to each bolus injection. Data were analyzed by Two-way
202 ANOVA (Group x Carotid body intact vs. denervated) for Angiotensin II or NaCN injection.
203 Holm-Sidak post-hoc test determined group differences.

204 *Serum angiotensin concentration*

205 Blood was collected after induction of IV anesthetic but before any drug infusion from the above
206 experiment from the femoral vein. Blood was left to coagulate for 20 minutes on ice then spun at

207 4,000rpm for 10 minutes at 4°C. Serum was drawn, aliquoted, snap-frozen, and stored at -80°C
208 until analysis. Angiotensin ELISA (Raybiotech #EIAR-ANGII-1) was used per manufacturer's
209 instructions. Groups (Control pups vs. perinatal nicotine-exposed pups) were analyzed with two-
210 sided unpaired t-test.

211 *Arterial pressure assessment between groups*

212 Rats from control or perinatal nicotine-exposed mothers were handled daily following weaning
213 at PND 21 and habituated to the tail plethysmography system (IITC Lifesciences). Three-minute
214 averages of tail cuff-measured blood pressure was averaged to attain a single value for each
215 animal. Data were compared using an unpaired two-sided t-test.

216 *Carotid body-mediated changes in arterial pressure*

217 Perinatal nicotine-exposed rats were prepared for telemetric implant between PND 56-60. Rats
218 were anesthetized with 5% isoflurane (balance O_2) as induction and maintained on a surgical
219 plane with 2-3% isoflurane. The abdominal area was isolated, shaved, and treated with 3x
220 betadyne and 3x 70% alcohol. A midline incision was made, and the descending aorta below the
221 renal arteries and renal nerves were isolated. The Kaha telemetry dual sympathetic nerve activity
222 /pressure (TRM56SP, AD Instruments) were instrumented around the renal nerves using
223 KwikGard dental impression material to isolate electrodes for renal sympathetic nerve activity
224 (RSNA) recording. The pressure transducer was inserted into the aorta as per manufacturer's
225 instructions to measure continuous pressure measurement. The surgical area was sewn in layers,
226 and the skin was secured with surgical staples. Rats were given buprenorphine (0.03mg/kg SQ)
227 2x daily for three days and allowed to recover for a total of 5 days before commencing recording.
228 Pressure and RSNA were recorded for 1 week; then rats were anesthetized as above; the neck
229 area was isolated, shaved, and treated with 3x betadine and 3x 70% alcohol. A midline incision

230 was made on the neck, and the carotid bodies were identified behind the occipital arteries. The
231 carotid sinus nerve was severed bilaterally, and the skin was sewn with subcuticular sutures.
232 Buprenorphine was delivered as above, and recording commenced for another week following
233 recovery. Arterial pressure waveforms delineated heart rate, systolic, diastolic, mean arterial
234 pressure, pulse pressure, and respiratory rate. RSNA was filtered, rectified, and integrated using
235 LabChart 8. Data were binned into daily averages and analyzed pre-post with a two-sided paired
236 t-test.

237 *Statistics*

238 Specific statistical tests are described for each experiment above. Data were averaged and
239 analyzed for each experiment as above. Data were analyzed using Graphpad v10.

240 **Results**

241 *Epigenetic changes in the carotid body in response to perinatal nicotine exposure*

242 To investigate possible genetic changes expounded by adverse maternal behaviors, we
243 implemented a standardized model of perinatal-nicotine exposure[28–30]. Given that the carotid
244 bodies are prime drivers of hypertension in self-actualized cardiometabolic disease states[22,36], we
245 conducted an unbiased transcriptomic screen of carotid bodies harvested from perinatal nicotine-
246 exposed pups on PND 56, 5 weeks after weaning and the final dose of nicotine delivered to the
247 mother. We pooled together carotid bodies from 5 pups in each group of nicotine-exposed and
248 saline control pups (Figure 1a). Samples were analyzed by sex, but no sex difference was found.
249 A total of 922 genes were differentially expressed between conditions, with 685 up-regulated,
250 237 down-regulated, and 19196 unchanged transcripts (Figure 1b, c). AgtR1a was significantly
251 upregulated in nicotine-exposed offspring compared to control (0.69 Log2 change, p_{adj}=0.04).

252 Angiotensin II type 2 receptor (AgtR2) was downregulated by perinatal nicotine exposure
253 (Log2FC=-3.246, p_{adj} =6.65x10^{-12}). No differences in angiotensinogen (Log2FC=0.233, p_{adj}
254 =0.693), angiotensin-converting enzyme (Log2FC=-0.071, p_{adj}=0.871), or renin (Log2FC=-
255 2.248, p_{adj}=0.645) were demonstrated (Supplementary data 2). Gene set enrichment analysis
256 (GSEA) was performed on the differentially expressed gene, revealing a vast number of highly
257 significant GO pathways, including GO:0004930 (normalized enrichment score =1.539;
258 Figure1d, Supplementary data 1), which included AgtR1a.

259 To validate these findings, we conducted immunohistochemistry and qPCR with taqman probes
260 to identify possible upregulation of potential signaling pathways in the carotid bodies between
261 perinatal nicotine exposed and control pups. We show that in relation to HPRT, AgtR1a was
262 significantly upregulated in perinatal nicotine-exposed offspring compared to control. AgtR2 and
263 TRPV1 transcription was not significantly increased (Supplementary figure 1).

264 To test whether changes in angiotensin signaling occurred outside the carotid bodies, we tested
265 whether RNA transcripts of AgtR1a, AgtR2, angiotensinogen, angiotensin-converting enzyme, or
266 renin were altered in the kidney and brains of perinatal nicotine exposed pups compared to
267 controls. We observed that angiotensinogen and angiotensin-converting enzymes were
268 significantly upregulated in the brains and kidneys of perinatal nicotine-exposed rats compared
269 to the control, and renin was downregulated in the kidneys of perinatal nicotine-exposed rats
270 compared to the control with no change in the brain (Supplementary figure 2). In contrast, both
271 AgtR1a and AgtR2 were unchanged in the brains and kidneys of perinatal nicotine-exposed rats
272 compared to control rats (Supplementary figure 2).

273 Given that our goal was to elucidate possible epigenetic differences responsible for mediating a
274 neurogenic form of hypertension, we probed further and conducted whole genome DNA bisulfite

275 sequencing[37] of the carotid bodies from perinatal nicotine-exposed and control pups on PND 56
276 (Figure 2a). Samples were analyzed by sex, but no sex difference was found. Mapping the whole
277 genome of the carotid bodies between groups revealed that the predominant changes to DNA
278 methylation occurred in the promoter (suppression) and intron/exon regions (enhancement,
279 Figure 2b). Methylation was distributed throughout the genome where a differential set of Genes
280 were altered predominantly on the cytosine-guanine (CG) and cytosine-
281 arginine/threonine/guanine-guanine (CHG) regions (Figure 2b). GO analyses of whole genes
282 (Figure 2d) and promoter regions (Figure 2e) revealed similar GO terms as with transcriptomic
283 changes. Importantly, a significant difference in methylation AgtR1a between groups was
284 demonstrated with a difference of 0.448319 between perinatal nicotine exposed and control rats
285 (Supplementary data 3). AgtR1 was orthogonally confirmed with immunoprecipitation of
286 methylated DNA compared to total DNA amplifying AgtR1 to assess global methylation (Figure
287 2c). AgtR1 DNA was not significantly methylated in brains but was increased in the kidneys of
288 perinatal nicotine-exposed rats compared to controls (Supplementary figure 3). Given that these
289 methylation changes occurred in regions associated with the upregulation of angiotensin GPCR
290 signaling, we wanted to investigate the functional outcomes of this pathway further. The
291 combined transcriptomic changes and DNA methylation of the whole genome point to an
292 upregulation of angiotensin signaling within the carotid bodies of perinatal nicotine-exposed
293 offspring.

294 Proteins for AgtR1, TRPV1, and tyrosine hydroxylase (a standard marker of carotid body glomus
295 cells) were all present in sections of carotid bodies harvested from perinatal nicotine-exposed
296 offspring where AgtR1 is on glomus cells, and TRPV1 appears to oppose glomus cells on the
297 post-synaptic terminals[38] (Supplementary figure 1), However, our resolution is insufficient to

298 determine the localization of glomus cells definitively. It is possible that these antibodies may
299 suffer from this lack of specificity in rats. As such, our staining may not reflect the accurate
300 location of AgtR1 in rat carotid body glomus cells. Nevertheless, given our RNAseq, qPCR, and
301 DNA methylation data, along with others who have orthogonally demonstrated the presence of
302 AgtR1 in glomus cells[38–41], we are confident of the expression and upregulation of AgtR1 in the
303 carotid bodies of perinatal nicotine exposed rats.

304 *Nicotine upregulates AgtR1 activity*

305 To show that nicotine itself is responsible for AgtR1 upregulation, we used a cell culture model.
306 PC12 cells have been routinely used as a surrogate carotid body glomus cell system[42–44]. Six
307 hours of nicotine exposure significantly upregulated AgtR1a gene expression (Figure 3a).
308 Differences in AgtR2 and TRPV1 were not demonstrated (Figure 3a). Differences in
309 angiotensinogen, angiotensin converting enzyme, renin, and regulatory genes of EPAS1 (Hif2α)
310 and tyrosine hydroxylase (TH- Figure 3a) were not demonstrated between conditions in relation
311 to the housekeeping gene HPRT. DNA methylation of AgtR1 was confirmed with the DNA
312 methylation pulldown assay (Figure 3b).

313 Using calcium imaging, we investigated how nicotine would augment glomus cell excitation. We
314 show that with 1 hour of exposure to nicotine, PC12 cells increased their level of calcium spike
315 frequency. The addition of angiotensin increased PC12 cell firing frequency to a level similar to
316 nicotine. Importantly, nicotine combined with angiotensin did not further increase PC12 cell
317 excitation. Further, losartan reduced calcium activity in PC12 cells when delivered to angiotensin
318 or nicotine + angiotensin-stimulated cells concurrently. The reduction in calcium flux was also
319 reduced with TRPV1 antagonist (AMG9810), and in combination with AMG9810 and Losartan
320 (Figure 3c). In conclusion, nicotine has a stimulatory effect on PC12 and, quite likely, carotid

321 body glomus cells to increase the expression and excitation of the angiotensin signaling pathway
322 via AgtR1 and TRPV1.

323 *Angiotensin acutely increases arterial pressure*

324 To assess acute carotid body reactivity to angiotensin, pups from perinatal nicotine-exposed or
325 control mothers were anesthetized and given a bolus angiotensin injection into the jugular vein
326 before and after acute carotid body denervation (Figure 4 a, b). In response to jugular vein
327 injected angiotensin (circulates through the pulmonary circulation, then encounters the carotid
328 bodies), arterial pressure was significantly elevated in nicotine-exposed offspring compared to
329 controls (Figure 4c, Supplementary figure 4). In response to sodium cyanide, which blocks
330 mitochondrial complex III and has been routinely used as a carotid body stimulant, there was no
331 significant difference between groups (Figure 4d, Supplementary figure 4). Following carotid
332 body denervation, arterial pressure was suppressed and did not respond to angiotensin or sodium
333 cyanide as vigorously (Figure 4c, d, Supplementary figure 4). The reactivity to angiotensin and
334 NaCN were attributed to the carotid bodies, however, given that boluses were delivered through
335 the jugular vein, off-target effects cannot be ruled out.

336 Importantly, serum harvested from these rats prior to any drug delivery demonstrated that
337 circulating levels of angiotensin were not altered between groups (Figure 4e), similar to previous
338 results[18]. It is possible that our analysis may be affected by background proteins in our sample,
339 despite the ability of angiotensin II ELISAs to discern various forms of angiotensin and cleaved
340 fragments[45].

341 These data demonstrate a significant increase in carotid body excitability in response to
342 angiotensin *in vivo* and suggest a hyperactive angiotensin signaling pathway within the carotid
343 bodies of perinatal nicotine-exposed offspring.

344 *Carotid bodies are responsible for elevated blood pressure in perinatal nicotine-exposed*
345 *offspring*

346 We evaluated arterial pressure between quiescent conscious control and nicotine-exposed
347 offspring using tail-cuff plethysmography on PND 56. Indeed, arterial pressure was higher in
348 nicotine-exposed offspring (Figure 5a). To definitively demonstrate that the carotid bodies were
349 primarily involved in perinatal nicotine-exposed hypertension, we implanted indwelling
350 telemetry to measure real-time arterial pressure from the aorta and efferent sympathetic activity
351 directed to the renal nerve between PND 56-60 (Figure 5b, Supplementary figure 5). We show
352 that within the same animal, carotid body denervation drastically reduces arterial pressure and
353 RSNA (Figure 5b, Supplementary figure 5). The reduction in arterial pressure with carotid body
354 denervation was predominantly due to the suppression of systolic pressure, which significantly
355 reduced pulse pressure (Supplementary figure 5). The reductions of RSNA as a result of carotid
356 body denervation also coincide with a reduced respiratory rate, similar to other models of
357 hypertension[19]. We attribute our changes in response to carotid body denervation to a reduction
358 of RSNA as measured and demonstrated by others[19,20]. However, we did not assess the precise
359 contribution of the carotid bodies to RSNA levels as previous[19]. Nevertheless, we note the
360 association of RSNA to respiratory rate, which indicates that the reduction of respiratory rate
361 following carotid body denervation would be tied to the fall in RSNA. These data demonstrate
362 that carotid body basal activity and excitation contribute to the hypertensive state in perinatal
363 nicotine-exposed offspring.

364 **Discussion**

365 Epigenetic changes in response to adverse maternal programming lead to cardiovascular
366 sequelae in later life. Hypertension has been a consistent outcome associated with many adverse

367 intra-uterine insults ranging from undernutrition[46,47], overnutrition[47,48], hypoxia[49,50], and stress[51].
368 The risk of hypertension is thought to be significantly increased in perinatal nicotine-exposed
369 offspring. The current data demonstrate that epigenetic changes in angiotensin signaling in the
370 carotid bodies mediate hypertension in perinatal nicotine-exposed offspring.

371 We show, for the first time, that epigenetic modifications in response to adverse maternal
372 programming in the form of nicotine exposure increase angiotensin, angiotensin II type 1a
373 receptor transcripts, and angiotensin II type 1 receptor DNA intron methylation, demonstrating
374 an increase in angiotensin signaling in the carotid bodies. These epigenetic changes *in vivo* are
375 confirmed *in vitro* as we show that nicotine directly increases AgtR1 gene expression, AgtR1
376 DNA methylation, and AgtR1 stimulation in PC12, glomus-like cells, in culture.

377 Importantly, the difference in epigenetic changes to AgtR1 was predominantly confined to
378 carotid bodies as the brain did not show an increase in gene expression or DNA methylation,
379 whereas kidneys only showed increased DNA methylation between perinatal nicotine exposed
380 and control pups. Angiotensinogen and angiotensin-converting enzyme gene expression was
381 upregulated in the brains and kidneys, and renin was increased in the kidneys of perinatal
382 nicotine exposed compared to control pups. In line with previous investigations, blood pressure
383 reactivity to angiotensin is increased through a neurogenic mechanism involving carotid body-
384 mediated excitation of efferent sympathetic activity. Finally, we showed, for the first time, that
385 carotid body denervation reduced blood pressure in perinatal nicotine-exposed rats alongside
386 efferent sympathetic activity.

387 Clinical data demonstrate that hypertension is likely in offspring that experienced intra-
388 uterine/perinatal smoke exposure[2,7,52–56]; however, the age, sex, and potential for additional
389 confounding lifestyle factors make it difficult to tease out this association, and measurements

390 beyond adolescence have not been completed to date. Pre-clinical data using rodent models show
391 that vascular reactivity to angiotensin via angiotensin II type 1 receptor gene expression, protein
392 expression, and signaling increases in aortae and mesenteric arterioles following prenatal and
393 perinatal nicotine exposure[14,15,18]. Accordingly, increased angiotensin II type 1 receptor activity,
394 RNA, and DNA methylation[57,58] have been consistent findings in response to perinatal nicotine-
395 exposed offspring in vascular tissues. Our data show that additional sensory neural systems,
396 which are significantly tied to hypertension[20], are also augmented and induce hypertension in
397 perinatal nicotine-exposed rats.

398 To date, scant data are available regarding the effects of nicotine exposure or perinatal nicotine
399 exposure on carotid body activity and resulting autonomic reflex disturbances[23,59]. Carotid bodies
400 are tasked with a multitude of homeostatic control mechanisms that regulate nutrient and oxygen
401 delivery to tissues[21]. Their role in blood pressure regulation is highlighted by genetic[22] and
402 epigenetic[27] modifications demonstrating the ability to increase basal activity and result in
403 augmented blood pressure. Specifically, the spontaneously hypertensive rat (SHR) has
404 augmented carotid body basal activity, which translates to alterations in breathing, blood pressure
405 regulation, and glucose homeostasis[22]. Importantly, these carotid body changes appear to hinge
406 on a significant difference in transcriptomic profile compared to their normotensive genetic
407 counterpart, the Wistar-Kyoto (WKY) rat[22]. Further, and particularly salient to the current
408 argument, carotid body denervation in SHR reduced arterial pressure and respiratory modulation,
409 whereas carotid body denervation in WKY rats had no effect[19]. Importantly, evidence
410 demonstrates that carotid body basal excitation can change via epigenetic modifications that
411 suppress redox disinhibition[27] to alter basal regulatory mechanisms such as breathing regulation.

412 A consistent finding is that intrauterine conditions with low oxygen[23] or hyperleptinemia[60] lead
413 to augmented carotid body basal activity. Therefore, it is possible that deficiencies in the
414 intrauterine environment augment arterial pressure in offspring due to the carotid body-regulated
415 mechanism. Our data are the first to demonstrate that adverse maternal programming leads to
416 carotid body epigenetic changes in AgtR1a and, importantly, the first to demonstrate that these
417 epigenetic changes occur as a result of genetic upregulation via DNA methylation, which results
418 in carotid body excitation. This carotid body excitation appears to be due to increased
419 angiotensin signaling within the carotid bodies due to increases in carotid body micro signaling
420 domains. Our *in vitro* experiments with PC12 cells demonstrate that epigenetic changes in
421 carotid body angiotensin signaling directly result from nicotine exposure. Further, the reactivity
422 of PC12 cells was regulated by nicotine to increase AgtR1 signaling. AgtR1 signaling in the
423 carotid bodies has been tied to a TRPV1-mediated mechanism in response to repeated hypoxic
424 bouts[38]. Given that losartan and TRPV1 blockade suppressed calcium signaling in PC12 cells,
425 with no further reduction in calcium excitation with dual inhibition, we suggest that a similar
426 mechanism is responsible for the augmentation of basal carotid body excitation. These data then
427 fit with the increased carotid body reactivity to angiotensin in an anesthetized preparation and the
428 consistent reduction in arterial pressure with carotid body denervation in conscious perinatal
429 nicotine-exposed offspring.

430 *Conclusion*

431 Hypertension resulting from perinatal nicotine exposure is due to epigenetic modifications within
432 the carotid bodies. The increased AgtR1-TRPV1 signaling increases efferent sympathetic activity
433 to augment arterial pressure. Future investigations should target neurogenic signaling
434 mechanisms to alleviate hypertension due to adverse epigenetic programming.

Perspectives

Carotid body denervation has shown clinical utility, as human clinical trials have shown that unilateral carotid body denervation results in a meaningful reduction in human blood pressure[61,62]. In fact, the reduction of systolic and diastolic arterial pressure with carotid body unilateral denervation[62,63] appears to be similar to renal denervation[64,65]. Targeting the carotid bodies offers the advantage of suppressing the first step of reflex blood pressure regulation (i.e., sensory afferents[64,65]. Therefore, we suggest that a targeted suppression or reversal of angiotensin signaling in the carotid bodies and renin-angiotensinogen and angiotensin-converting enzyme in the kidneys would help alleviate increased blood pressure and cardiac afterload and limit unwanted side effects by standard drug therapies or invasive procedures.

Acknowledgements and sources of funding

This project was supported by T32IP4707 of the Regents of the University of California Tobacco-Related Diseases Research Program (TRDRP). NJ is supported by NIH grant R21AI159221, R56AI175328, UCLA CTSI UL1TR001881-01 and, T32KT4708 of the Regents of the University of California TRDRP. WY is supported by NIH grant P50HD098593 and R01HD099924. VR is supported by NIH grant R01HL151769 and IR00737, T32IP5044, T32IR5048, and T32IR5365 of the Regents of the University of California TRDRP. The content is solely the responsibility of the authors and does not necessarily represent the official views of the National Institutes of Health or the UCOP TRDRP. Figures, 1a, 2a, 4a and 6a,b were completed with Biorender under a CC-BY-NC-ND license.

Author contributions

F.Z. Z.W.& J.K. contributed to experimental design, conducted experiments and analyzed data. H.M, K.D. and J.L. contributed to experimental execution and data analysis. W.Y. and V.R. assisted with experimental design and analysis. N.J. designed the study, conducted experiments, analyzed data, and prepared the manuscript and figures. All authors agree on the manuscript.

Disclosures

All authors do not declare competing interests.

References

1. Higa R, Leonardi ML, Jawerbaum A. Intrauterine Programming of Cardiovascular Diseases in Maternal Diabetes. Front Physiol [Internet]. 2021 [cited 2024 Jan 11];12. Available from: https://www.frontiersin.org/articles/10.3389/fphys.2021.760251

2. Parada-Ricart E, Luque V, Zaragoza M, Ferre N, Closa-Monasterolo R, Koletzko B, Grote V, Gruszfeld D, Verduci E, Xhonneux A, Escribano J. Effect of maternal smoking during pregnancy on child blood pressure in a European cohort. Sci Rep. Nature Publishing Group; 2022 Oct 15;12(1):17308.

3. Palinski W. Effect of Maternal Cardiovascular Conditions and Risk Factors on Offspring Cardiovascular Disease. Circulation. American Heart Association; 2014 May 20;129(20):2066–2077.

4. Dasinger JH, Davis GK, Newsome AD, Alexander BT. Developmental Programming of Hypertension. Hypertension. American Heart Association; 2016 Oct;68(4):826–831.

5. Alexander BT, Dasinger JH, Intapad S. Fetal Programming and Cardiovascular Pathology. Compr Physiol. 2015 Apr;5(2):997–1025. PMCID: PMC4772789

6. Taylor L, Kelly B, Leeson P. Maternal Smoking and Infant Cardiovascular Physiology. Hypertension. American Heart Association; 2010 Mar;55(3):614–616.

7. Kooijman MN, Bakker H, Franco OH, Hofman A, Taal HR, Jaddoe VWV. Fetal Smoke Exposure and Kidney Outcomes in School-Aged Children. Am J Kidney Dis Off J Natl Kidney Found. 2015 Sep;66(3):412–420. PMID: 25641064

8. Nordenstam F. Prenatal nicotine exposure was associated with long-term impact on the cardiovascular system and regulation—Review. Acta Paediatr. John Wiley & Sons, Ltd; 2021 Sep 1;110(9):2536–2544.

9. Nordenstam F, Norman M, Caidahl K, Wickström R. Arterial Stiffness and Carotid Intima-Media Thickness in Children Exposed to Smokeless Tobacco in Fetal Life. J Am Heart Assoc. Wiley; 2024 Jan 16;13(2):e9128.

10. Spindel ER, McEvoy CT. The Role of Nicotine in the Effects of Maternal Smoking during Pregnancy on Lung Development and Childhood Respiratory Disease. Implications for Dangers of E-Cigarettes. Am J Respir Crit Care Med. 2016 Mar 1;193(5):486–494. PMCID: PMC4824926

11. Oakes JM, Fuchs RM, Gardner JD, Lazartigues E, Yue X. Nicotine and the renin-angiotensin system. Am J Physiol - Regul Integr Comp Physiol. 2018 Nov 1;315(5):R895–R906. PMCID: PMC6295500

12. Ramalingam A, Budin SB, Mohd. Fauzi N, Ritchie RH, Zainalabidin S. Angiotensin II Type I Receptor Antagonism Attenuates Nicotine-Induced Cardiac Remodeling, Dysfunction, and Aggravation of Myocardial Ischemia-Reperfusion Injury in Rats. Front Pharmacol [Internet]. 2019 [cited 2024 Jan 25];10. Available from: https://www.frontiersin.org/articles/10.3389/fphar.2019.01493

13. Fried ND, Morris TM, Whitehead A, Lazartigues E, Yue X, Gardner JD. Angiotensin II type 1 receptor mediates pulmonary hypertension and right ventricular remodeling induced by inhaled nicotine. Am J Physiol Heart Circ Physiol. 2021 Apr 1;320(4):H1526–H1534. PMCID: PMC8260386

14. Mao C, Zhang H, Xiao D, Zhu L, Ding Y, Zhang Y, Wu L, Xu Z, Zhang L. Perinatal nicotine exposure alters AT1 and AT2 receptor expression pattern in the brain of fetal and offspring rats. Brain Res. 2008 Dec 3;1243:47–52. PMCID: PMC2664080

15. Xiao D, Huang X, Lawrence J, Yang S, Zhang L. Fetal and Neonatal Nicotine Exposure Differentially Regulates Vascular Contractility in Adult Male and Female Offspring. J Pharmacol Exp Ther. American Society for Pharmacology and Experimental Therapeutics; 2007 Feb 1;320(2):654–661. PMID: 17068201

16. Gao YJ, Holloway AC, Su LY, Takemori K, Lu C, Lee RMKW. Effects of fetal and neonatal exposure to nicotine on blood pressure and perivascular adipose tissue function in adult life. Eur J Pharmacol. 2008 Aug 20;590(1):264–268.

17. Paxton WG, Marrero MB, Klein JD, Delafontaine P, Berk BC, Bernstein KE. The angiotensin II AT1 receptor is tyrosine and serine phosphorylated and can serve as a substrate for the src family of tyrosine kinases. Biochem Biophys Res Commun. 1994 Apr 15;200(1):260–267. PMID: 7513159

18. Tao H, Rui C, Zheng J, Tang J, Wu L, Shi A, Chen N, He R, Wu C, Li J, Yin X, Zhang P, Zhu Z, Tao J, Xiao J, Mao C, Xu Z. Angiotensin II-mediated vascular changes in aged offspring rats exposed to perinatal nicotine. Peptides. 2013 Jun 1;44:111–119.

19. Abdala AP, McBryde FD, Marina N, Hendy EB, Engelman ZJ, Fudim M, Sobotka PA, Gourine AV, Paton JF. Hypertension is critically dependent on the carotid body input in the spontaneously hypertensive rat. J Physiol. 2012 Sep 1;590(Pt 17):4269–77. PMID: 22687617

528 20. McBryde FD, Abdala AP, Hendy EB, Pijacka W, Marvar P, Moraes DJ, Sobotka PA, Paton
529 JF. The carotid body as a putative therapeutic target for the treatment of neurogenic
530 hypertension. Nat Commun. 2013;4:2395.

531 21. Zera T, Moraes DJA, da Silva MP, Fisher JP, Paton JFR. The Logic of Carotid Body
532 Connectivity to the Brain. Physiology. 2019 Jun 5;34(4):264–282. PMID: 31165684

533 22. Pauza AG, Thakkar P, Tasic T, Felippe I, Bishop P, Greenwood MP, Rysevaite-Kyguoliene
534 K, Ast J, Broichhagen J, Hodson DJ, Salgado HC, Pauza DH, Japundzic-Zigon N, Paton
535 JFR, Murphy D. GLP1R Attenuates Sympathetic Response to High Glucose via Carotid
536 Body Inhibition. Circ Res. 2022 Mar 4;130(5):694–707. PMCID: PMC8893134

537 23. Stéphan-Blanchard E, Chardon K, Léké A, Delanaud S, Djeddi D, Libert JP, Bach V, Telliez
538 F. In Utero Exposure to Smoking and Peripheral Chemoreceptor Function in Preterm
539 Neonates. Pediatrics. American Academy of Pediatrics; 2010 Mar 1;125(3):e592–e599.
540 PMID: 20176675

541 24. Argacha JF, Xhaët O, Gujic M, Adamopoulos D, Beloka S, Dreyfuss C, Degaute JP, van de
542 Borne P. Nicotine increases chemoreflex sensitivity to hypoxia in non-smokers. J
543 Hypertens. 2008 Feb;26(2):284–294. PMID: 18192843

544 25. Holgert H, Hökfelt T, Hertzberg T, Lagercrantz H. Functional and developmental studies of
545 the peripheral arterial chemoreceptors in rat: effects of nicotine and possible relation to
546 sudden infant death syndrome. Proc Natl Acad Sci U S A. 1995 Aug 1;92(16):7575–7579.
547 PMCID: PMC41382

548 26. Prieto-Lloret J, Caceres AI, Obeso A, Rocher A, Rigual R, Agapito MT, Bustamante R,
549 Castañeda J, Perez-Garcia MT, Lopez-Lopez JR, Gonzalez C. Ventilatory responses and
550 carotid body function in adult rats perinatally exposed to hyperoxia. J Physiol. 2004 Jan
551 1;554(Pt 1):126–144. PMCID: PMC1664733

552 27. Nanduri J, Prabhakar NR. Epigenetic regulation of Carotid Body Oxygen Sensing: Clinical
553 Implications. Adv Exp Med Biol. 2015;860:1–8. PMCID: PMC4870818

554 28. Liu J, Yu C, Doherty TM, Akbari O, Allard P, Rehan VK. Perinatal nicotine exposure-
555 induced transgenerational asthma: Effects of reexposure in F1 gestation. FASEB J Off
556 Publ Fed Am Soc Exp Biol. 2020 Sep;34(9):11444–11459. PMCID: PMC7839813

557 29. Xiao D, Huang X, Li Y, Dasgupta C, Wang L, Zhang L. Antenatal Antioxidant Prevents
558 Nicotine-Mediated Hypertensive Response in Rat Adult Offspring. Biol Reprod. 2015
559 Sep;93(3):66. PMCID: PMC4710188

560 30. Wongtrakool C, Wang N, Hyde DM, Roman J, Spindel ER. Prenatal Nicotine Exposure
561 Alters Lung Function and Airway Geometry through α7 Nicotinic Receptors. Am J Respir
562 Cell Mol Biol. 2012 May;46(5):695–702. PMCID: PMC3359906

563 31. Wang Z, McSwiggin H, Newkirk SJ, Wang Y, Oliver D, Tang C, Lee S, Wang S, Yuan S,
564 Zheng H, Ye P, An W, Yan W. Insertion of a chimeric retrotransposon sequence in mouse
565 Axin1 locus causes metastable kinky tail phenotype. Mob DNA. 2019 May 3;10(1):17.
566 PMID: 31073336

567 32. Lisanti S, von Zglinicki T, Mathers JC. Standardization and quality controls for the
568 methylated DNA immunoprecipitation technique. Epigenetics. Taylor & Francis; 2012 Jun
569 1;7(6):615–625. PMID: 22507898

570 33. Jendzjowsky NG, Roy A, Wilson RJA. Asthmatic allergen inhalation sensitises carotid
571 bodies to lysophosphatidic acid. J Neuroinflammation. 2021 Aug 31;18:191. PMCID:
572 PMC8408927

573 34. Jendzjowsky NG, Roy A, Barioni NO, Kelly MM, Green FHY, Wyatt CN, Pye RL, Tenorio-
574 Lopes L, Wilson RJA. Preventing acute asthmatic symptoms by targeting a neuronal
575 mechanism involving carotid body lysophosphatidic acid receptors. Nat Commun. 2018
576 Oct 2;9(1):4030. PMID: 30279412 PMCID: PMC6168495

577 35. Marshall JM. Interactions between local dilator and sympathetic vasoconstrictor influences
578 in skeletal muscle in acute and chronic hypoxia. Exp Physiol. 2015 Dec 1;100(12):1400–
579 1411.

580 36. Conde SV, Sacramento JF, Guarino MP. Carotid body: a metabolic sensor implicated in
581 insulin resistance. Physiol Genomics. 2018 01;50(3):208–214. PMID: 29373079

582 37. Kurdyukov S, Bullock M. DNA Methylation Analysis: Choosing the Right Method. Biology.
583 2016 Jan 6;5(1):3. PMCID: PMC4810160

584 38. Roy A, Farnham MMJ, Derakhshan F, Pilowsky PM, Wilson RJA. Acute intermittent
585 hypoxia with concurrent hypercapnia evokes P2X and TRPV1 receptor-dependent sensory
586 long-term facilitation in naïve carotid bodies. J Physiol. :n/a-n/a.

587 39. Schultz HD. Angiotensin and Carotid Body Chemoreception in Heart Failure. Curr Opin
588 Pharmacol. 2011 Apr;11(2):144–149. PMCID: PMC3075378

589 40. Lam SY, Liu Y, Ng KM, Liong EC, Tipoe GL, Leung PS, Fung ML. Upregulation of a local
590 renin-angiotensin system in the rat carotid body during chronic intermittent hypoxia. Exp
591 Physiol. 2014 Jan;99(1):220–231. PMID: 24036592

592 41. M-L Fung null, Lam SY, Dong X, Chen Y, Leung PS. Postnatal hypoxemia increases
593 angiotensin II sensitivity and up-regulates AT1a angiotensin receptors in rat carotid body
594 chemoreceptors. J Endocrinol. 2002 May;173(2):305–313. PMID: 12010638

595 42. Hockman D, Adameyko I, Kaucka M, Barraud P, Otani T, Hunt A, Hartwig AC, Sock E,
596 Waithe D, Franck MCM, Ernfors P, Ehinger S, Howard MJ, Brown N, Reese J, Baker CVH.
597 Striking parallels between carotid body glomus cell and adrenal chromaffin cell
598 development. Dev Biol. 2018 May 25; PMID: 29807017

599 43. Dixon DN, Loxley RA, Barron A, Cleary S, Phillips JK. Comparative studies of PC12 and
600 mouse pheochromocytoma-derived rodent cell lines as models for the study of
601 neuroendocrine systems. In Vitro Cell Dev Biol Anim. 2005 Aug;41(7):197–206. PMID:
602 16223334

603 44. Zhu WH, Conforti L, Czyzyk-Krzeska MF, Millhorn DE. Membrane depolarization in PC-12
604 cells during hypoxia is regulated by an O2-sensitive K+ current. Am J Physiol. 1996
605 Aug;271(2 Pt 1):C658-665. PMID: 8770007

45. Chappell MC. Biochemical evaluation of the renin-angiotensin system: the good, bad, and absolute? Am J Physiol - Heart Circ Physiol. American Physiological Society; 2016 Jan 1;310(2):H137. PMID: 26475588

46. Mariano VS, Boer PA, Gontijo JAR. Fetal Undernutrition Programming, Sympathetic Nerve Activity, and Arterial Hypertension Development. Front Physiol [Internet]. 2021 [cited 2024 Feb 6];12. Available from: https://www.frontiersin.org/journals/physiology/articles/10.3389/fphys.2021.704819

47. Eriksson J, Forsén T, Tuomilehto J, Osmond C, Barker D. Fetal and Childhood Growth and Hypertension in Adult Life. Hypertension. American Heart Association; 2000 Nov;36(5):790–794.

48. Cho NH, Silverman BL, Rizzo TA, Metzger BE. Correlations between the intrauterine metabolic environment and blood pressure in adolescent offspring of diabetic mothers. J Pediatr. 2000 May 1;136(5):587–592.

49. Walton SL, Bielefeldt-Ohmann H, Singh RR, Li J, Paravicini TM, Little MH, Moritz KM. Prenatal hypoxia leads to hypertension, renal renin-angiotensin system activation and exacerbates salt-induced pathology in a sex-specific manner. Sci Rep. Nature Publishing Group; 2017 Aug 15;7(1):8241.

50. Zhou J, Xiao D, Hu Y, Wang Z, Paradis A, Mata-Greenwood E, Zhang L. Gestational Hypoxia Induces Preeclampsia-Like Symptoms via Heightened Endothelin-1 Signaling in Pregnant Rats. Hypertension. American Heart Association; 2013 Sep;62(3):599–607.

51. Costa TJ, De Oliveira JC, Giachini FR, Lima VV, Tostes RC, Bomfim GF. Programming of Vascular Dysfunction by Maternal Stress: Immune System Implications. Front Physiol [Internet]. 2022 [cited 2024 Feb 6];13. Available from: https://www.frontiersin.org/journals/physiology/articles/10.3389/fphys.2022.787617

52. Mourino N, Varela-Lema L, Ahluwalia JS, Rey-Brandariz J, Candal-Pedreira C, Ruano-Ravina A, Vila-Farinas A, Torres A, Pérez-Rios M. Maternal smoking in pregnancy and blood pressure during childhood and adolescence: a meta-analysis. Eur J Pediatr. 2023;182(5):2119–2132. PMCID: PMC10175379

53. He B, Zhang Q, Guo Y, Ao Y, Tie K, Xiao H, Chen L, Xu D, Wang H. Prenatal smoke (Nicotine) exposure and offspring's metabolic disease susceptibility in adulthood. Food Chem Toxicol. 2022 Oct 1;168:113384.

54. Hacke C, Weisser B. Effects of Parental Smoking on Exercise Systolic Blood Pressure in Adolescents. J Am Heart Assoc. Wiley; 2015 May 11;4(5):e001936.

55. Aryanpur M, Yousefifard M, Oraii A, Heydari G, Kazempour-Dizaji M, Sharifi H, Hosseini M, Jamaati H. Effect of passive exposure to cigarette smoke on blood pressure in children and adolescents: a meta-analysis of epidemiologic studies. BMC Pediatr. 2019 May 21;19:161. PMCID: PMC6528314

56. Liu SH, Liu B, Sanders AP, Saland J, Wilson KM. Secondhand smoke exposure and higher blood pressure in children and adolescents participating in NHANES. Prev Med. 2020 May;134:106052. PMCID: PMC8025403

646 57. Li Y, Xiao D, Dasgupta C, Xiong F, Tong W, Yang S, Zhang L. Perinatal Nicotine Exposure
647 Increases Vulnerability of Hypoxic-Ischemic Brain Injury in Neonatal Rats: Role of
648 Angiotensin II Receptors. Stroke J Cereb Circ. 2012 Sep;43(9):2483–2490. PMCID:
649 PMC3429721

650 58. Demura M, Demura Y, Takeda Y, Saijoh K. Dynamic regulation of the angiotensinogen
651 gene by DNA methylation, which is influenced by various stimuli experienced in daily life.
652 Hypertens Res. Nature Publishing Group; 2015 Aug;38(8):519–527.

653 59. Stéphan-Blanchard E, Bach V, Telliez F, Chardon K. Perinatal nicotine/smoking exposure
654 and carotid chemoreceptors during development. Respir Physiol Neurobiol. 2013 Jan
655 1;185(1):110–119. PMID: 22743051

656 60. Dos Santos E, Sacramento JF, Melo BF, Conde SV. Carotid Body Dysfunction in Diet-
657 Induced Insulin Resistance Is Associated with Alterations in Its Morphology. Adv Exp Med
658 Biol. 2018;1071:103–108. PMID: 30357740

659 61. Narkiewicz K, Ratcliffe LEK, Hart EC, Briant LJB, Chrostowska M, Wolf J, Szyndler A,
660 Hering D, Abdala AP, Manghat N, Burchell AE, Durant C, Lobo MD, Sobotka PA, Patel NK,
661 Leiter JC, Engelman ZJ, Nightingale AK, Paton JFR. Unilateral Carotid Body Resection
662 in Resistant Hypertension: A Safety and Feasibility Trial. JACC Basic Transl Sci. 2016 Aug
663 1;1(5):313–324.

664 62. Niewinski P, Janczak D, Rucinski A, Tubek S, Engelman ZJ, Piesiak P, Jazwiec P,
665 Banasiak W, Fudim M, Sobotka PA, Javaheri S, Hart ECJ, Paton JFR, Ponikowski P.
666 Carotid body resection for sympathetic modulation in systolic heart failure: results from
667 first-in-man study. Eur J Heart Fail. 2017;19(3):391–400.

668 63. Schlaich M, Schultz C, Shetty S, Hering D, Worthley S, Delacroix S, Reddy V, Sievert H,
669 Zeller T, Noory E, Boehm M, Mahfoud F, Malek F, Kmonicek P, Neuzil P. 1416Transvenous
670 carotid body ablation for resistant hypertension: main results of a multicentre safety and
671 proof-of-principle cohort study. Eur Heart J. 2018 Aug 1;39(suppl_1):ehy565.1416.

672 64. Sesa-Ashton G, Nolde JM, Muente I, Carnagarin R, Lee R, Macefield VG, Dawood T, Sata
673 Y, Lambert EA, Lambert GW, Walton A, Kiuchi MG, Esler MD, Schlaich MP. Catheter-
674 Based Renal Denervation: 9-Year Follow-Up Data on Safety and Blood Pressure
675 Reduction in Patients With Resistant Hypertension. Hypertension. American Heart
676 Association; 2023 Apr;80(4):811–819.

677 65. Jami O, Tijani Y, Et-tahir A. Device-Based Therapy for Resistant Hypertension: An Up-to-
678 Date Review. High Blood Press Cardiovasc Prev. Nature Publishing Group;
679 2022;29(6):537. PMID: 36178479

680

681 **Figure legends**

682 **Figure 1. Perinatal nicotine exposure alters RNA transcripts associated with angiotensin**

683 **signaling in the carotid body. a)** Transcriptomic study design. Nicotine or saline was delivered

684 to the mother on estrous day 7 (E7) to post-natal day (PND) 21. Bilateral carotid body (CB)
685 samples were micro-dissected from perinatal nicotine or saline (control) exposed rats on PND
686 56. (n=5 rats per group- tissues were pooled to yield sufficient RNA for analysis) Two male and
687 Two female groups per condition. **b)** Principal component analysis (PCA) plot showing distinct
688 separation between nicotine and control groups. PCA1 was group and PCA2 was sex. **c)**
689 Heatmap showing overall differences in RNA distribution. **d)** Gene set enrichment analysis
690 (GSEA) plot for G-protein-coupled receptor activity (0004930) where AgtR1a was significantly
691 increased in nicotine-exposed offspring compared to controls.

692 **Figure 2. Perinatal nicotine exposure alters DNA methylation in the carotid body. a)** DNA-
693 methylation study design. Nicotine or saline was delivered to the mother on estrous day 7 (E7) to
694 post-natal day (PND) 21. Bilateral carotid body (CB) samples were micro-dissected from
695 perinatal nicotine or saline (control) exposed rats on PND 56. (n=5 rats per group- tissues were
696 pooled to yield sufficient DNA for analysis). One male and one female group per condition. **b)**
697 Heatmap displaying cytosine-guanine (C-G) and cytosine-arginine/threonine/guanine-guanine
698 (CHG) methylation differences in carotid bodies between nicotine and saline-exposed rats.
699 Mapping of methylation changes is confined to the CG and CHG regions as per the heat maps. **c)**
700 Immunoprecipitation of methylated DNA compared to whole DNA demonstrates an increase of
701 methylated AgtR1 DNA in the carotid bodies of nicotine exposed compared to control offspring.
702 ΔCT was used to compare differences between groups (lower value equals greater amount of
703 methylation). **d)** Enriched gene ontology (GO) terms for C-G methylated DNA between nicotine-
704 exposed and control pups. **e)** Dot plot showing the gene number and enrichment factor of GO
705 pathways between nicotine-exposed and control pups.

706 **Figure 3. Nicotine increases AgtR1 pathway in cultured PC12 cells. a)** PC12 cells (rat adrenal
707 pheochromocytoma cells, resemble carotid body glomus cells) were cultured for 6 hours with
708 and without 50µg/ml nicotine (similar concentration to a single dose of nicotine used *in vivo*), **a)**
709 angiotensin II type 1a receptor (AgtR1a) was increased by nicotine (T_{28}=2.299) The calculated
710 increase of AgtR1a was 100.3% in comparison to control. Angiotensin II type 2 receptor
711 (AgtR2) (T_{28}=0.5307), transient receptor potential vanilloid 1 (TRPV1) (T_{28}=0.2589),
712 angiotensin converting enzyme (ACE, T_{16}=0.4231), angiotensinogen (T_{16}=1.056), renin
713 (T_{16}=0.1950), and regulatory genes of endothelial PAS domain-containing protein 1/ hypoxia
714 inducible factor 2 alpha (EPAS1/Hif2α; T_{28}=0.3774) and Tyrosine hydroxylase (TH- common
715 PC12 and glomus cell marker, T_{28}=0.6274) were unchanged. Data presented as ΔCT compared to
716 Hypoxanthine-guanine phosphoribosyltransferase (HPRT) housekeeping gene. **b)** AgtR1 DNA
717 was hypermethylated in PC12 cells following 6 hours of nicotine exposure. (T_{10}=3.881). **c)** PC12
718 cells were cultured for 1 hour with media (control) nicotine (Nic, 50µg/ml), Angiotensin (Ang-
719 50ng/ml), Nic + Ang, Ang+Losartan (AII1R blockade 3µM), Nic+Ang+Losartan, Ang+TRPV1
720 antagonist (TRPV1x, AMG9810 10µM), Nic+Ang+TRPV1x, Ang+Losartan+TRPV1x, and
721 Nic+Ang+Losartan+TRPV1x and imaged for calcium flux using Incucyte calcium imaging with
722 Calcium Orange (forms Calcium esther complex- non-ratiometric imaging). One-way ANOVA
723 ($F_{9,54}$=5.225, $p<0.0001$) Holm-Sidak post-hoc test, p-values inset in figure.

724 **Figure 4. Carotid body reactivity to angiotensin is increased in perinatal nicotine-exposed**
725 **pups compared to control with unaltered serum angiotensin. a)** Diagram of *in vivo*
726 experimental preparation- serum was isolated before injection of angiotensin or sodium cyanide
727 (NaCN). **b)** A representative trace of arterial pressure of vehicle and perinatal nicotine-exposed
728 pups on post-natal day (PND) 56 in response to a bolus jugular vein IV injection of angiotensin.

729 **c)** The absolute increase in arterial pressure in response to angiotensin in vehicle (grey) and
730 perinatal-nicotine exposed pups (red) before and following carotid body denervation $F_{1,}$
731 $_{11}$=11.34). **d)** The absolute increase in arterial pressure in response to NaCN in vehicle (grey) and
732 perinatal-nicotine exposed pups (red) before and following carotid body denervation $F_{1,}$
733 $_{11}$=2.364). **e)** Serum was harvested before administration of bolus injections (T_{14}=0.8077).

734 **Figure 5. Perinatal nicotine-exposed rats have increased mean arterial pressure mediated**
735 **by carotid body augmentation of sympathetic activity. a**) Mean arterial pressure (MAP), as
736 assessed by tail-cuff plethysmography, was augmented in nicotine-exposed offspring compared
737 to controls (T_{20}=7.964). N=11 per group, 2 independent experiments. **b**) Perinatal nicotine-
738 exposed pups were implanted with radio telemetry to measure arterial pressure and renal
739 sympathetic nerve activity (RSNA) on PND 56 as per Figure1a. Arterial pressure and renal
740 sympathetic nerve activity was recorded for 7 days, and then carotid bodies were denervated and
741 recordings recommenced for an additional 7 days. Raw traces of arterial pressure (AP) and
742 efferent renal sympathetic nerve activity (vasoconstrictor outflow to kidneys) before carotid body
743 denervation (Carotid body intact- BEFORE) and following carotid body denervation (Carotid
744 body denervated- AFTER) in a representative perinatal nicotine exposed rat using telemetry.
745 Summary statistics in n=5 perinatal nicotine rats comparing the absolute change of MAP and
746 RSNA. MAP (T_4=3.568), RSNA (T_4=4.762).

747

Figure 1.

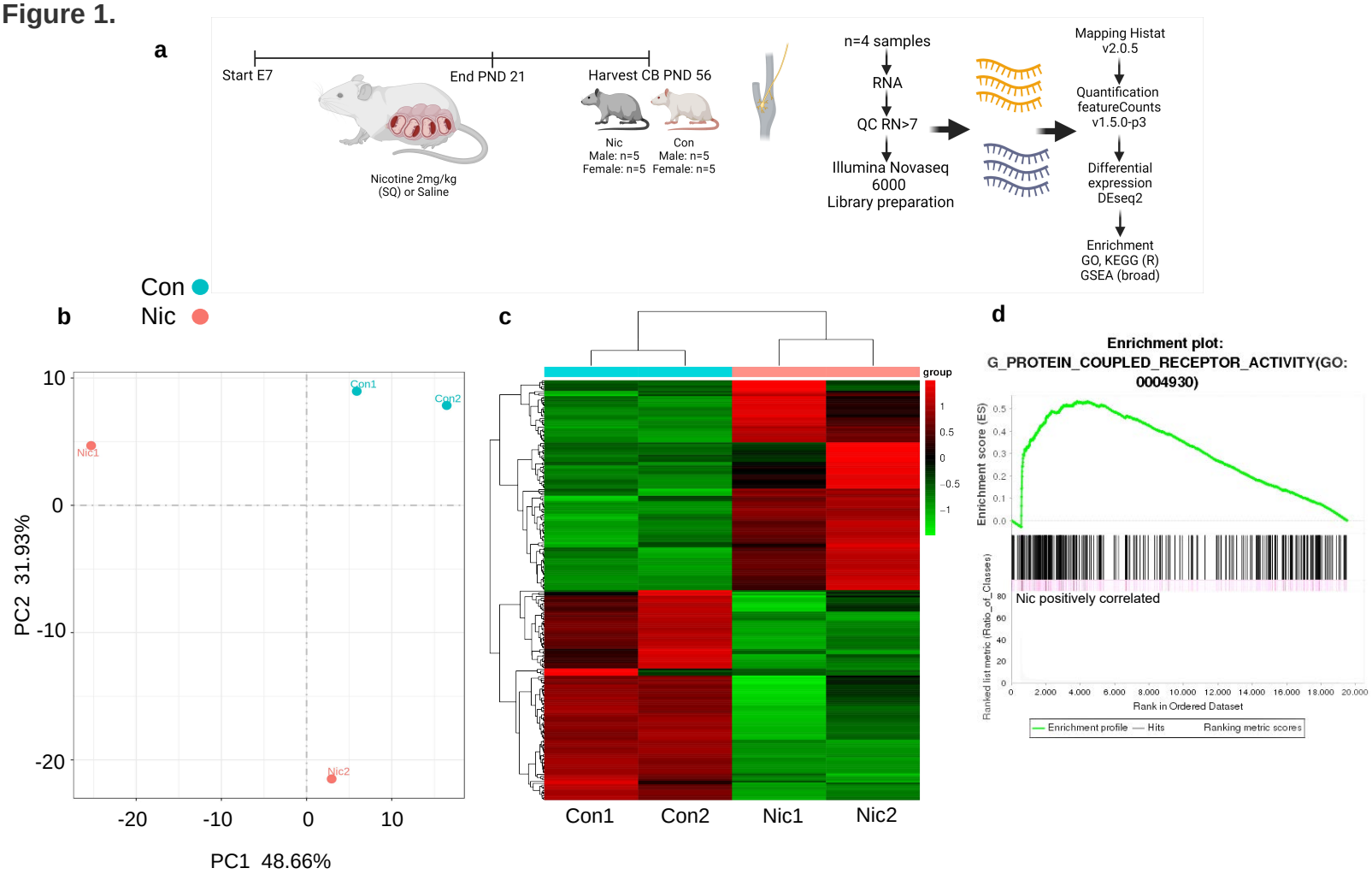
a
Start E7
End PND 21
Harvest CB PND 56
Nicotine 2mg/kg
(SQ) or Saline
Nic
Male: n=5
Female: n=5
Con
Male: n=5
Female: n=5
n=4 samples
RNA
QC RN>7
Illumina Novaseq
6000
Library preparation
Mapping Histat
v2.0.5
Quantification
featureCounts
v1.5.0-p3
Differential
expression
DEseq2
Enrichment
GO, KEGG (R)
GSEA (broad)
Con
Nic
b
Con1
Con2
Nic1
Nic2
PC2 31.93%
PC1 48.66%
c
group
Con1
Con2
Nic1
Nic2
d
Enrichment plot:
G_PROTEIN_COUPLED_RECEPTOR_ACTIVITY(GO:
0004930)
Enrichment score (ES)
Nic positively correlated
Ranked list metric (Ratio_of_Classes)
Rank in Ordered Dataset
Enrichment profile
Hits
Ranking metric scores

Figure 2.

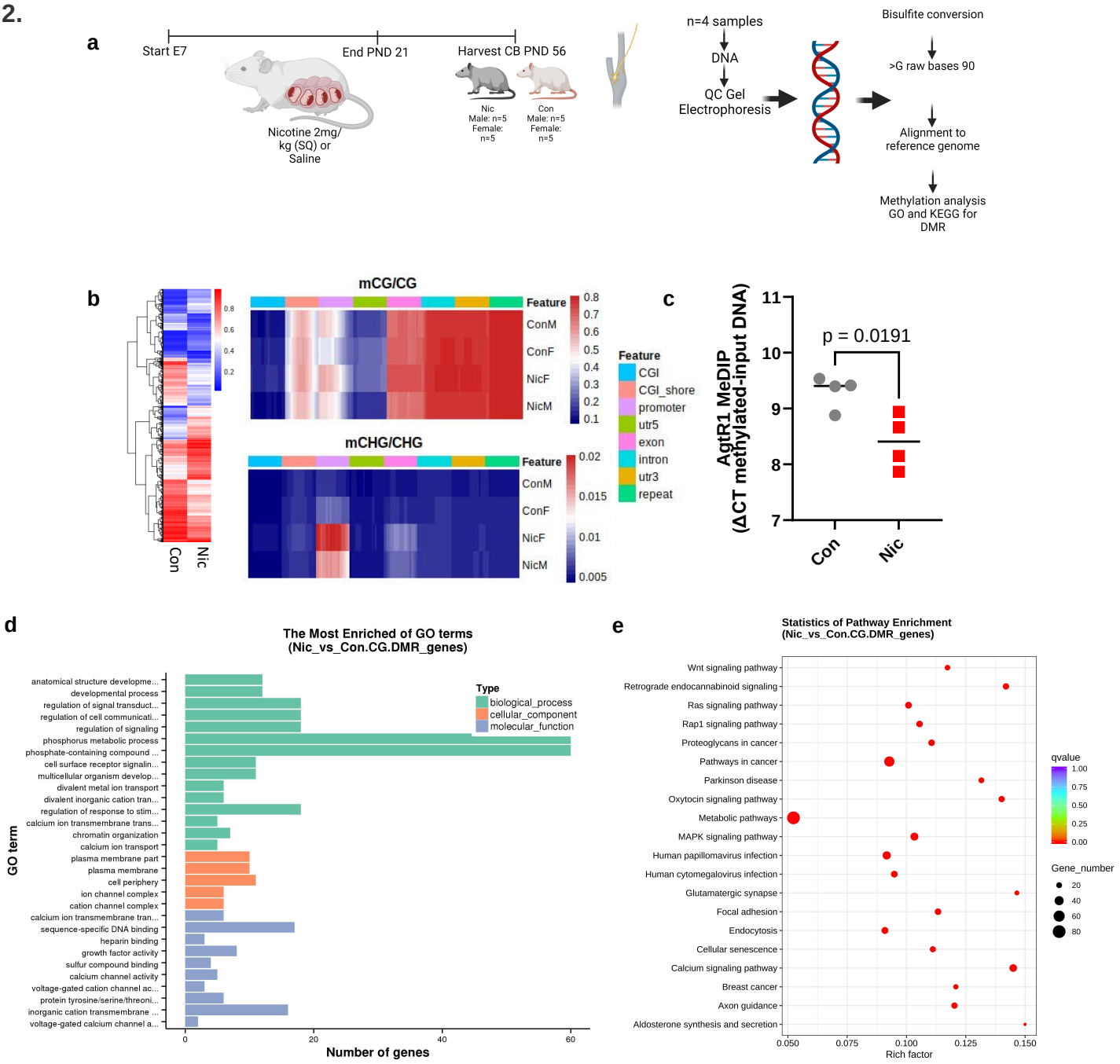
a
Start E7
End PND 21
Harvest CB PND 56
Nicotine 2mg/ kg (SQ) or Saline
Nic Male: n=5 Female: n=5
Con Male: n=5 Female: n=5
n=4 samples
DNA
QC Gel Electrophoresis
Bisulfite conversion
>G raw bases 90
Alignment to reference genome
Methylation analysis GO and KEGG for DMR
b
mCG/CG
mCHG/CHG
Feature
ConM
ConF
NicF
NicM
Con
Nic
Feature
CGI
CGI_shore
promoter
utr5
exon
intron
utr3
repeat
c
AgtR1 MeDIP (ΔCT methylated-input DNA)
p = 0.0191
Con
Nic
d
The Most Enriched of GO terms (Nic_vs_Con.CG.DMR_genes)
GO term
Number of genes
Type
biological_process
cellular_component
molecular_function
anatomical structure developme...
developmental process
regulation of signal transduct...
regulation of cell communicati...
regulation of signaling
phosphorus metabolic process
phosphate-containing compound ...
cell surface receptor signalin...
multicellular organism develop...
divalent metal ion transport
divalent inorganic cation tran...
regulation of response to stim...
calcium ion transmembrane trans...
chromatin organization
calcium ion transport
plasma membrane part
plasma membrane
cell periphery
ion channel complex
cation channel complex
calcium ion transmembrane tran...
sequence-specific DNA binding
heparin binding
growth factor activity
sulfur compound binding
calcium channel activity
voltage-gated cation channel ac...
protein tyrosine/serine/threoni...
inorganic cation transmembrane ...
voltage-gated calcium channel a...
e
Statistics of Pathway Enrichment (Nic_vs_Con.CG.DMR_genes)
Wnt signaling pathway
Retrograde endocannabinoid signaling
Ras signaling pathway
Rap1 signaling pathway
Proteoglycans in cancer
Pathways in cancer
Parkinson disease
Oxytocin signaling pathway
Metabolic pathways
MAPK signaling pathway
Human papillomavirus infection
Human cytomegalovirus infection
Glutamatergic synapse
Focal adhesion
Endocytosis
Cellular senescence
Calcium signaling pathway
Breast cancer
Axon guidance
Aldosterone synthesis and secretion
Rich factor
qvalue
Gene_number

Figure 3.

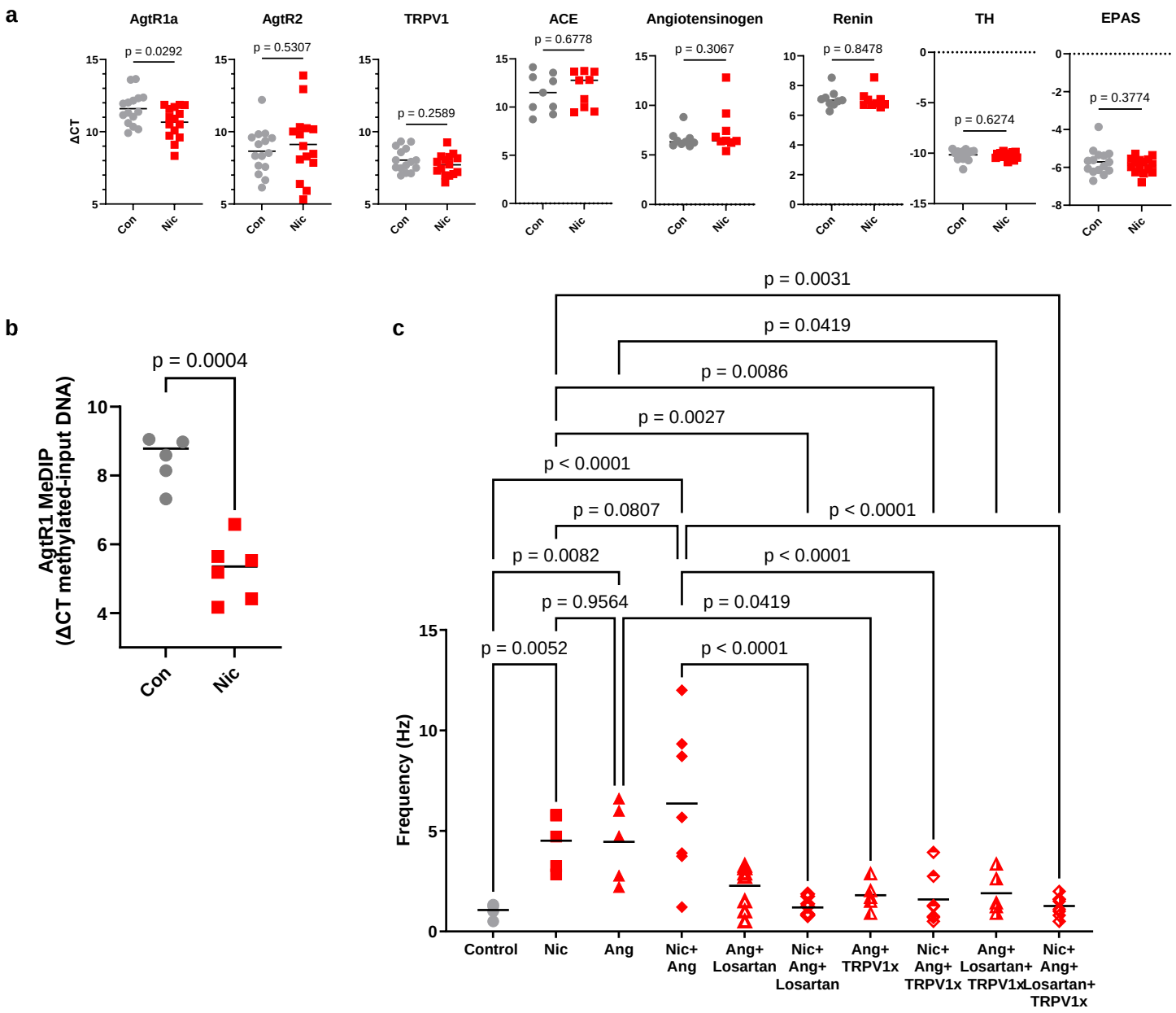
a
AgtR1a
AgtR2
TRPV1
ACE
Angiotensinogen
Renin
TH
EPAS
ΔCT
p = 0.0292
p = 0.5307
p = 0.2589
p = 0.6778
p = 0.3067
p = 0.8478
p = 0.6274
p = 0.3774
Con
Nic
b
AgtR1 MeDIP
(ΔCT methylated-input DNA)
p = 0.0004
Con
Nic
c
Frequency (Hz)
p = 0.0031
p = 0.0419
p = 0.0086
p = 0.0027
p < 0.0001
p = 0.0807
p < 0.0001
p = 0.0082
p < 0.0001
p = 0.9564
p = 0.0419
p = 0.0052
p < 0.0001
Control
Nic
Ang
Nic+ Ang
Ang+ Losartan
Nic+ Ang+ Losartan
Ang+ TRPV1x
Nic+ Ang+ TRPV1x
Ang+ Losartan+ TRPV1x
Nic+ Ang+ Losartan+ TRPV1x

Figure 4.

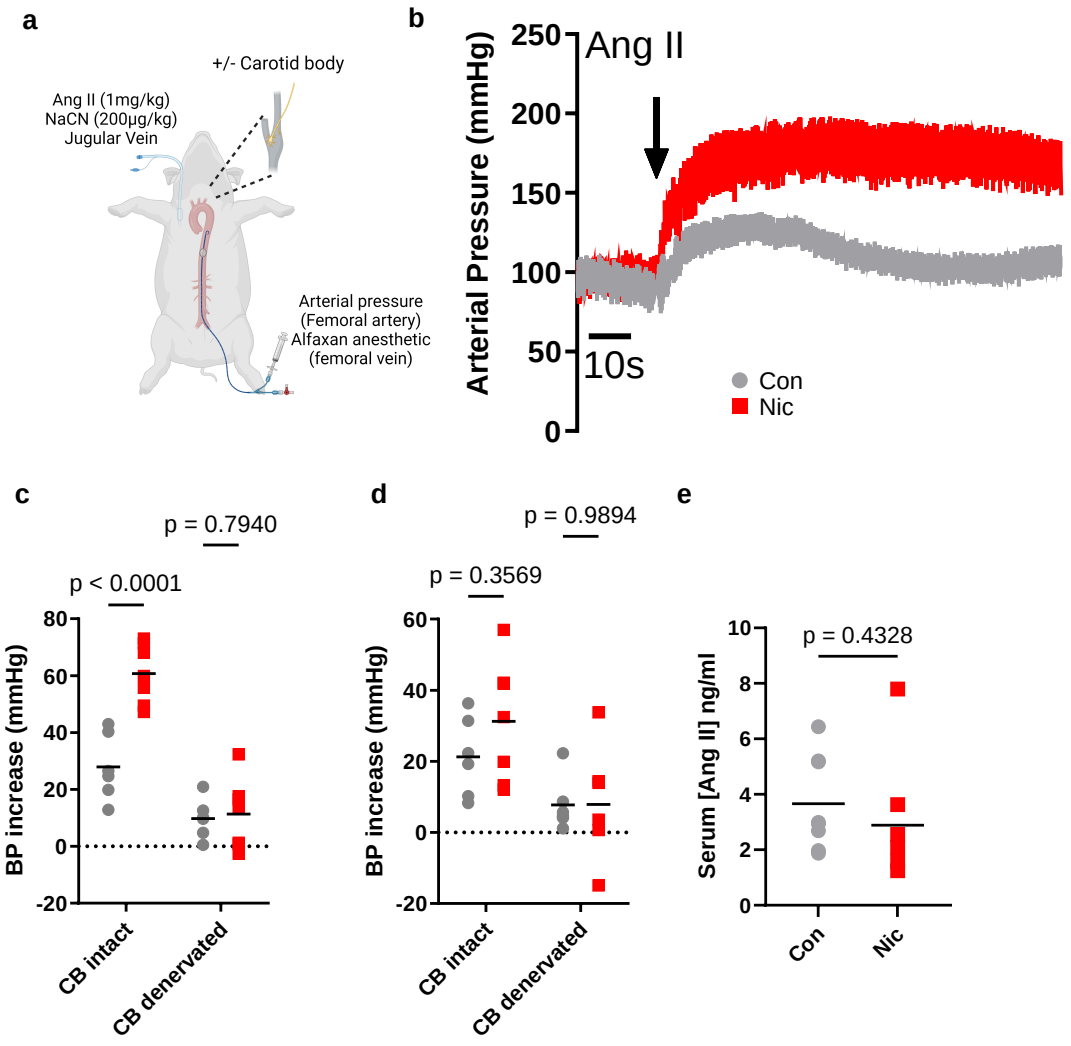
a
+/- Carotid body
Ang II (1mg/kg)
NaCN (200µg/kg)
Jugular Vein
Arterial pressure
(Femoral artery)
Alfaxan anesthetic
(femoral vein)
b
Ang II
Arterial Pressure (mmHg)
250
200
150
100
50
0
10s
Con
Nic
c
p = 0.7940
p < 0.0001
BP increase (mmHg)
80
60
40
20
0
-20
CB intact
CB denervated
d
p = 0.9894
p = 0.3569
BP increase (mmHg)
60
40
20
0
-20
CB intact
CB denervated
e
p = 0.4328
Serum [Ang II] ng/ml
10
8
6
4
2
0
Con
Nic

Figure 5.

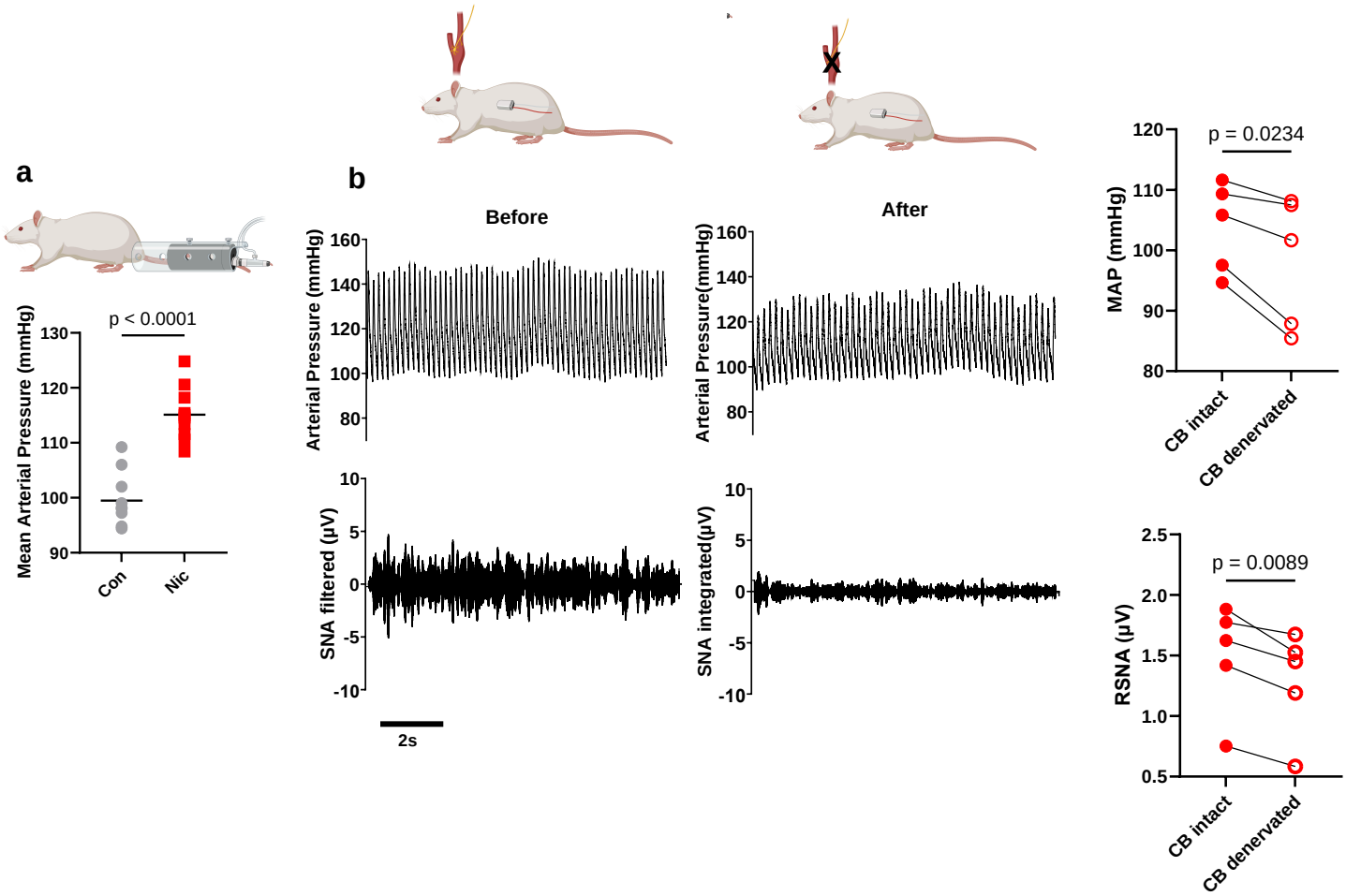
a
b
Mean Arterial Pressure (mmHg)
p < 0.0001
130
120
110
100
90
Con
Nic
Before
After
Arterial Pressure (mmHg)
Arterial Pressure(mmHg)
160
140
120
100
80
SNA filtered (µV)
SNA integrated(µV)
10
5
0
-5
-10
2s
MAP (mmHg)
p = 0.0234
CB intact
CB denervated
RSNA (µV)
p = 0.0089
2.5
2.0
1.5
1.0
0.5